

Cuprophilic Interactions in Luminescent Copper(I) Clusters with Bridging Bis(dicyclohexylphosphino)methane and Iodide Ligands: Spectroscopic and Structural Investigations

Wen-Fu Fu,^{*,[a, b, c]} Xin Gan,^[c] Chi-Ming Che,^{*,[b]} Qian-Yong Cao,^[a]
Zhong-Yong Zhou,^[d] and N. Nian-Yong Zhu^[b]

Abstract: Polynuclear copper(I) complexes with bridging bis(dicyclohexylphosphino)methane (dcpm) and iodide ligands, $[\text{Cu}_2(\text{dcpm})_2(\text{CH}_3\text{CN})_2](\text{BF}_4)_2$ (**1**), $[\text{Cu}_2(\text{dcpm})_2](\text{BF}_4)_2$ (**2**), $[(\text{CuI})_3(\text{dcpm})_2]$ (**3**), $[(\text{CuI})_4(\text{dcpm})_2]$ (**4**), and $[(\text{CuI})_2(\text{dcpm})_2]$ (**5**) were prepared and their structures determined by X-ray crystal analysis. The shortest Cu–Cu distance found in these complexes is 2.475(1) Å for **3**. Powdered samples of **1**, **3**, **4**, and **5** display intense and long-lived phosphorescence with

λ_{max} at 460, 626, 590, and 456 nm and emission quantum yields of 0.26, 0.11, 0.12, and 0.56 at room temperature, respectively. In the solid state, **2** displays both a weak emission at 377 and an intense one at 474 nm with an overall emission yield 0.42. The difference in

emission properties among complexes **1–5** suggests that both Cu–Cu interaction and coordination around the copper(I) center affect the excited state properties. A degassed solution of **2** in acetone gives a bright red emission with λ_{max} at 625 nm at room temperature. The difference absorption spectra of the triplet excited states of **1–5** in acetonitrile show broad absorption peaks at 340–410 and 850–870 nm.

Keywords: coordination chemistry • copper • luminescence • metal–metal interactions • polynuclear complexes

Introduction

Polynuclear copper(I) complexes have attracted considerable attention for their diverse structural and rich photoluminescent properties and potential applications in materials science.^[1–6] The structures of the copper(I) complexes formed by coordinating phosphine or bulky nitrogen base ligands to CuX had been described previously.^[7–12] These complexes are polynuclear copper(I) species with μ_2 -, μ_3 -, or μ_4 -bridging X atoms, and their structures are affected by the phosphine ligand and method of preparation. They display multiple emissive triplet excited states. Extensive studies by Ford and co-workers established that the higher energy emissions of $[\text{Cu}_4\text{X}_4\text{L}_4]$ (L = 2-(diphenylmethyl)pyridine or pyridine) come from halide-to-ligand charge transfer (XLCT) excited states, and the lower energy emission from an excited state with a mixture of XMCT (halide-to-metal charge-transfer) and MC (metal-centered) orbital parentage.^[13] Despite the fact that a d^{10} – d^{10} interaction is well documented in gold(I) systems^[14] and $\text{Cu}^1\cdots\text{Cu}^1$ separations as short as 2.35 Å have been reported for a long time,^[15] the existence of a weak bonding interaction between copper(I) atoms remains controversial.^[6b,16] In polynuclear complexes the chelate and bridging ligand plays an important role in fine-tuning the $\text{Cu}^1\cdots\text{Cu}^1$ contact distances, which affect the spectroscopic

[a] Prof. Dr. W.-F. Fu, Q.-Y. Cao
Technical Institute of Physics and Chemistry
Chinese Academy of Science, Peking 100101 (China)
Fax: (+86)10-64879375
E-mail: fuwf@ipc.ac.cn

[b] Prof. Dr. W.-F. Fu, Prof. Dr. C.-M. Che, Dr. N. N.-Y. Zhu
Department of Chemistry and HKU-CAS Joint Laboratory on New Materials
The University of Hong Kong, Pokfulam Road, Hong Kong SAR (China)
Fax: (+852)28571586
E-mail: fuwf@ipc.ac.cn
cmche@hku.hk

[c] Prof. Dr. W.-F. Fu, X. Gan
College of Chemistry and Chemical Engineering
Yunnan Normal University, Kunming 650092 (China)
Fax: (+86)871-5516061
E-mail: fuwf@ipc.ac.cn

[d] Prof. Dr. Z.-Y. Zhou
Department of Applied Biology and Chemical Technology
The Hong Kong Polytechnic University, Hong Hum, Hong Kong SAR (China)

Supporting information for this article is available on the WWW under <http://www.chemeurj.org/> or from the author.

properties. Several theoretical papers on binuclear copper(I) complexes were unresponsive of the existence of the Cu^I–Cu^I bonding interaction, but a recent investigation on Cu₂O based on electron and X-ray diffraction experiments provided evidence for the existence of such bonding interactions.^[17] In previous work, we reported spectroscopic evidence for Cu^I–Cu^I interactions in [Cu₂(dcpm)₂]Y₂ (Y = ClO₄[−] and PF₆[−]; dcpm = bis(dicyclohexylphosphino)methane) solids.^[6b] In the present study we prepared [Cu₂(dcpm)₂(CH₃CN)₂](BF₄)₂ (**1**), [Cu₂(dcpm)₂](BF₄)₂ (**2**), [(CuI)₃(dcpm)₂] (**3**), [(CuI)₄(dcpm)₂] (**4**), and [(CuI)₂(dcpm)₂] (**5**) and examined their structures and photophysical properties. The results suggest that the Cu^I–Cu^I distances and the ligands and coordination number around the copper(I) center play key roles in affecting photophysical properties of polynuclear copper(I) complexes.

Results and Discussion

Comparison of crystal structures: The structures of the copper(I) halide compounds with phosphine or bulky nitrogen base ligands usually have tetrahedrally coordinated Cu^I sites with the tetrahedral faces capped by halide and/or and other ligands.^[18] A series of copper(I) compounds exhibiting “cubane” tetranuclear structure, such as [Cu₄X₄L₄] (L = pyridine, substituted pyridine, or a saturated amine) complexes, have been reported previously.^[13,19] These polynuclear copper(I) compounds exhibit a “stairstep” configuration having square (Cu₂X₂) units that form the steps of the stairs.^[20] In the case of [(C₆H₅)₃PCuX]₄, as the halide changes from Cl[−] to Br[−] and I[−], the structure changes from a cubane core to a single “step” tetranuclear structure. In addition, the steric influence of the bulky coordinated ligand can control the structure.^[21] As depicted in Figure 1, the binuclear copper(I) complex [Cu₂(dcpm)₂](BF₄)₂ (**2**) was obtained in high yield upon stirring a mixture of [Cu(CH₃CN)₄]BF₄ and dcpm in a 1:1 ratio in dichloromethane. Crystal structure analysis of **2** reveals the P1–Cu1–P2 bond angle to be 168.2° rather than 180° as expected for an idealized two-coordinate linear geometry. Presumably, this is due to the BF₄[−] ion, which interacts very weakly with Cu^I through one fluorine atom (Tables 1 and 2). Although the Cu⋯F(BF₄[−]) distance of 2.803 Å is approximately 0.14 Å less than the estimated sum of the van der Waals radii of copper and fluorine atoms, it is considerably greater than the value of 1.89 Å for the sum of the ionic radii of the

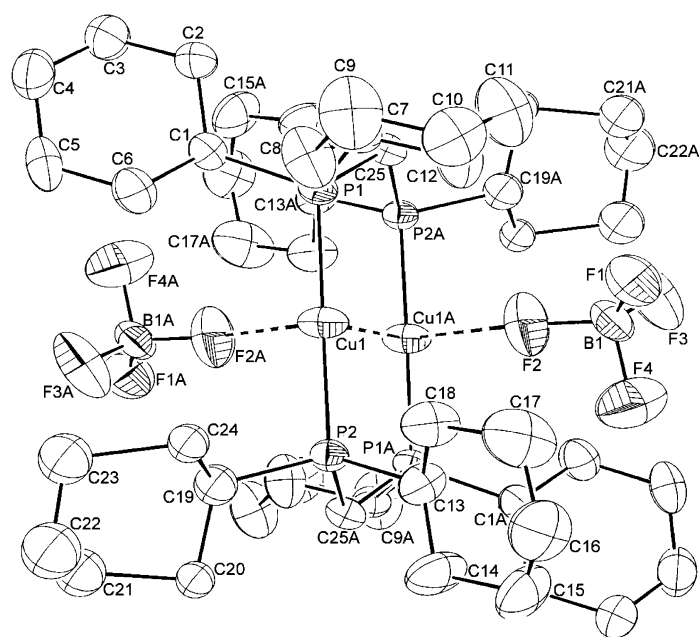


Figure 1. Structure of [Cu₂(dcpm)₂](BF₄)₂ (perspective drawing; the thermal ellipsoids are drawn at 40% probability). The closest Cu⋯F (BF₄[−]) distance is 2.803(1) Å.

Table 1. Selected crystallographic and data collection parameters for complexes **1–4**.

	1	2	3	4
formula	(C ₅₄ H ₉₈ Cu ₂ N ₂ P ₄)·2(BF ₄)	(C ₅₀ H ₉₂ Cu ₂ P ₄)·2(BF ₄)	C ₁₀₄ H ₁₉₆ Cl ₄ Cu ₆ I ₆ O ₂ P ₈	C ₅₀ H ₉₂ Cu ₄ I ₄ P ₄
M _r	1199.22	1117.82	3010.81	1578.88
T (K)	301(2)	301(2)	294(2)	294(2)
crystal system	monoclinic	monoclinic	triclinic	triclinic
space group	P2 ₁ /n	C2/c	P1	P1
a [Å]	21.648(4)	24.078(5)	14.370(4)	10.328(2)
b [Å]	13.093(3)	13.813(3)	21.876(6)	11.709(2)
c [Å]	22.632(5)	17.686(4)	22.505(6)	13.929(2)
α [°]	90	90	108.068(7)	97.386(3)
β [°]	105.80(3)	106.99(3)	108.380(7)	110.354(3)
γ [°]	90	90	100.113(6)	102.243(3)
V [Å ³]	6173(2)	5625.6(19)	6083(3)	1505.2(4)
Z	4	4	2	1
ρ _{calcd} [Mg m ^{−3}]	1.291	1.320	1.644	1.742
μ (Mo Kα) [mm ^{−1}]	0.852	0.928	2.789	3.582
crystal size [mm]	0.25 × 0.20 × 0.15	0.40 × 0.3 × 0.15	0.28 × 0.22 × 0.20	0.20 × 0.18 × 0.12
F(000)	2544	2368	3032	780
2θ _{max} [°]	50.9	51.0	55.2	55.1
unique reflections	28 949	8718	41 392	10 203
parameters	649	292	1110	280
R _f	0.060	0.063	0.064	0.042
R _w	0.163	0.183	0.102	0.111
goodness of fit	0.96	1.10	0.96	1.03
residual electron density [e Å ^{−3}]	0.709/−0.783	0.657/−0.575	0.987/−0.921	0.982/−0.937

Cu⁺ and F[−] ions,^[22] which can be compared with the Y-shaped trigonal configuration of [(CuI)₂(dcpm)₂] (Figure 2). The complex [Cu₂(dcpm)₂](BF₄)₂ has a short intra-metal Cu⋯Cu separation (2.6905 Å), whereas [Cu₂(dcpm)₂(CH₃CN)₂](BF₄)₂ exhibits a distance of 2.8095 Å and adopts a Y-shaped trigonal configuration with P1–Cu1–P3, N1–Cu1–P1, and N1–Cu1–P3 bond angles of 145.0, 111.9, and 102.8°, respectively.

The reaction of CuI with dcpm (3:2 molar ratio) gave **3** in which both three- and four-coordinate Cu^I were found. Se-

Table 2. Selected bond lengths [Å] and bond angles [°] of **1–4**.

Complex 1									
Cu1–Cu2	2.810(1)	Cu1–P1	2.261(2)	Cu1–P3	2.270(2)	Cu1–N1	2.015(6)	Cu2–P2	2.260(2)
Cu2–P4	2.270(2)	Cu2–N2	2.096(6)	C51–N1	1.139(8)	C53–N2	1.133(8)		
N1–Cu1–P1	111.9(2)	N1–Cu1–P3	102.8(2)	P1–Cu1–P3	145.03(6)	N1–Cu1–Cu2	98.5(2)	P1–Cu1–Cu2	91.60(5)
P3–Cu1–Cu2	87.23(5)	N2–Cu2–P2	103.2(2)	N2–Cu2–P4	102.3(2)	P2–Cu2–P4	152.16(7)	N2–Cu2–Cu1	105.2(2)
P2–Cu2–Cu1	90.92(5)	P4–Cu2–Cu1	93.03(5)	C51–N1–Cu1	175.5(5)	C53–N2–Cu2	169.6(7)		
Complex 2									
Cu1–Cu1*	2.691(2)	Cu1–P1	2.216(1)	Cu1–P2*	2.224(1)	Cu1*–P2	2.224(1)	Cu–F	2.803(1)
B1–F1	1.325(9)	B1–F2	1.345(7)	B1–F3	1.37(1)	B1–F4	1.390(9)		
P1–Cu1–P2*	168.20(6)	P1–Cu1–Cu1*	97.74(5)	P2*–Cu1–Cu1*	92.27(5)	C1–P1–Cu1	111.6(2)	C25–P1–Cu1	111.9(1)
C7–P1–Cu1	114.9(2)	C25–P2–Cu1*	115.1(2)	C19–P2–Cu1*	104.8(4)	C13–P2–Cu1*	110.4(2)	F1–B1–F2	114.8(7)
F2–B1–F3	109.0(7)	F2–B1–F4	100.7(5)						
Complex 3									
Cu1–Cu2	2.9846(9)	Cu2–Cu3	2.4866(9)	Cu5–Cu6	2.475(1)	I1–Cu1	2.7625(8)	I1–Cu2	2.890(1)
I1–Cu3	2.6703(8)	I2–Cu1	2.794(1)	I2–Cu2	2.7510(9)	I3–Cu2	2.6178(8)	I3–Cu3	2.5689(8)
I4–Cu4	2.7819(9)	I4–Cu5	2.7425(8)	I4–Cu6	2.9501(8)	I5–Cu4	2.7905(8)	I5–Cu5	2.897(1)
I5–Cu6	2.7345(9)	I6–Cu5	2.6124(9)	I6–Cu6	2.6124(9)	Cu1–P1	2.296(1)	Cu1–P2	2.279(1)
Cu2–P3	2.197(1)	Cu3–P4	2.201(1)	Cu3–I1–Cu1	71.73(2)	Cu3–I1–Cu2	52.95(2)	Cu1–I1–Cu2	63.70(2)
Cu2–I2–Cu1	65.13(2)	Cu3–I3–Cu2	57.29(2)	I1–Cu1–I2	110.20(2)	Cu5–I4–Cu4	69.23(2)	Cu4–I4–Cu6	65.73(2)
Cu5–I4–Cu6	51.38(2)	Cu5–I5–Cu4	66.94(2)	Cu5–I5–Cu6	52.04(2)	Cu4–I5–Cu6	68.60(2)	Cu5–I6–Cu6	56.63(2)
I4–Cu4–I5	107.01(2)	P5–Cu4–P6	138.96(4)	P2–Cu1–P1	138.02(4)	P2–Cu1–I1	102.61(4)	P1–Cu1–I1	102.60(4)
P2–Cu1–I2	99.35(3)	P1–Cu1–I2	102.68(3)	I1–Cu1–I2	110.20(2)	P2–Cu1–Cu2	133.29(3)	P1–Cu1–Cu2	88.51(4)
I1–Cu1–Cu2	60.23(2)	I2–Cu1–Cu2	56.75(2)	P3–Cu2–Cu3	164.42(4)	P3–Cu2–I3	132.73(4)	Cu3–Cu2–I3	60.37(2)
P3–Cu2–I2	106.28(4)	Cu3–Cu2–I2	74.25(3)	I3–Cu2–I2	103.25(2)	P3–Cu2–I1	107.09(4)	Cu3–Cu2–I1	58.99(2)
I3–Cu2–I1	97.82(3)	I2–Cu2–I1	107.75(2)	P3–Cu2–Cu1	96.27(4)	Cu3–Cu2–Cu1	70.50(3)	I3–Cu2–Cu1	130.78(3)
I2–Cu2–Cu1	58.12(2)	I1–Cu2–Cu1	56.07(2)	P4–Cu3–Cu2	150.39(4)	P4–Cu3–I3	138.01(3)	Cu2–Cu3–I3	62.35(2)
P4–Cu3–I1	112.60(4)	Cu2–Cu3–I1	68.06(2)	I3–Cu3–I1	104.92(3)	C25–P1–Cu1	114.5(1)	C7–P1–Cu1	114.1(1)
Complex 4									
Cu1–Cu2	3.005 (1)	Cu1–Cu2*	2.5760(8)	Cu2–Cu1*	2.5758(6)	I1–Cu1	2.7983(8)	I1–Cu2	2.8057(8)
I1–Cu1*	2.8272(8)	I1–Cu2*	2.8806(8)	I2–Cu2*	2.6150(8)	I2–Cu1	2.6303(7)	Cu1–P1	2.2236(8)
Cu1–I1*	2.8272(8)	Cu2–P2	2.218 (1)	Cu2–I2*	2.6150(8)	Cu2–I1*	2.8806(8)	P1–C25	1.844(4)
P1–C7	1.848(4)	Cu2*–Cu1–Cu2	91.28(3)	Cu1*–Cu2–Cu1	88.72(3)	Cu1–I1–Cu2	64.86(2)	Cu1–I1–Cu1*	88.18(2)
Cu2–I1–Cu1*	54.43(2)	Cu1–I1–Cu2*	53.93(2)	Cu2–I1–Cu2*	89.45(2)	Cu1–I1–Cu2*	63.54(2)	Cu2*–I2–Cu1	58.83(2)
P1–Cu1–Cu2*	173.83(3)	P1–Cu1–I2	117.56(4)	Cu2*–Cu1–I2	60.29(2)	P1–Cu1–I1	121.30(4)	Cu2*–Cu1–I1	64.67(2)
I2–Cu1–I1	102.65(3)	P1–Cu1–I1*	114.32(4)	Cu2*–Cu1–I1*	62.36(2)	I2–Cu1–I1*	105.34(3)	I1–Cu1–I1*	91.82(2)
P1–Cu1–Cu2	91.09(3)	I2–Cu1–Cu2	151.35(3)	I1–Cu1–Cu2	57.69(2)	I1*–Cu1–Cu2	59.10(2)	P2–Cu1–Cu2*	179.34(5)
P2–Cu2–I2*	118.71(4)	Cu1*–Cu2–I2*	60.88(2)	P2–Cu2–I1	116.66(4)	Cu1*–Cu2–I1	63.21(2)	I2*–Cu2–I1	106.37(2)
P2–Cu2–I1*	119.25(4)	Cu1*–Cu2–I1*	61.41(2)	I2*–Cu2–I1*	100.86(2)	I1–Cu2–I1*	90.55(2)	P2–Cu2–Cu1	91.72(3)
I2*–Cu2–Cu1	149.39(3)	I1–Cu2–Cu1	57.45(2)	I1*–Cu2–Cu1	57.38(2)	C25–P1–C7	106.4(2)	C25–P1–C1	101.3(2)
C7–P1–C1	108.9(2)	C25–P1–Cu1	113.1(1)	C7–P1–Cu1	111.6(1)	C1–P1–Cu1	114.7 (1)	C25–P2–C13	102.4(2)
C25–P2–C19	99.9(1)	C13–P2–C19	106.1(2)	C25–P2–Cu2	114.9(1)	C13–P2–Cu2	115.7(1)	C19–P2–Cu2	115.9(1)

lected crystallographic data are listed in Tables 1 and 2. A perspective view of the structure is depicted in Figure 3. Two kinds of Cu–I interactions found; one I^- ion adopts a μ_3 -coordination mode that is similar to $(CuI)_3(dppm)_2^{[23]}$ in which three Cu atoms are in a trigonal-planar array with two I^- ions (I4 an I5) above and below the plane. Three sides of the triangle are bridged by the third iodine atom (I6) and dcpm ligands, the closest Cu...Cu contact being 2.4748 Å. The other consists of a triangular array of Cu atoms, connected by a μ_3 -I ligand above the plane of copper atoms. The I1 atom binds to the copper atoms with bond lengths of 2.6703 (I1–Cu3), 2.7625 (I1–Cu1), and 2.890 Å (I1–Cu2), whereas only two of the three copper atoms are bonded by a Cu1–I2–Cu2 linkage below the plane with a Cu1...Cu2 distance of 2.9846 Å and a Cu1–I2–Cu2 bond angle of 65.13°. One side of the triangle is bridged by a third iodine atom with a significantly shorter copper–copper separation of 2.4866 Å and a Cu(2)–I(3)–Cu(3) bond angle of 57.29°. Each of the other two edges is connected by a dcpm ligand. The Cu–P bond lengths are affected by the number of phosphorus atoms coordinated to the same

copper atom: Cu1–P1 = 2.296 Å for copper atoms with two coordinated phosphorus atoms; Cu2–P3 = 2.197 Å and Cu3–P4 = 2.201 Å for copper atoms with one coordinated phosphorus atom.

A perspective view of $[(CuI)_4(dcpm)_2]$ (**4**) is shown in Figure 4. Selected bond lengths and angles are given in Tables 1 and 2. The four copper atoms are arranged in a rectangular array with copper–copper distances of 3.0051–2.5758 Å. The copper atoms are tetracoordinate. The dcpm and iodide ligands bridge each edge of the Cu_4 plane to form a $Cu_4P_4I_2$ core. The dicapping iodide ligands are bonded to the four copper atoms in a μ_4 -fashion from opposite faces of the rectangle. The Cu–I bond lengths in quadruple bridging vary from 2.7979 to 2.8804 Å, which are significantly longer than double-bridging bond lengths of 2.6150 and 2.6303 Å (Figure 4).

Electron absorption spectra: The UV/Vis absorption spectral data for **1** to **5** in acetonitrile or dichloromethane are listed in Table 3. For **3** to **5**, no absorption band in the visible range has been observed, and the absorption spectra in

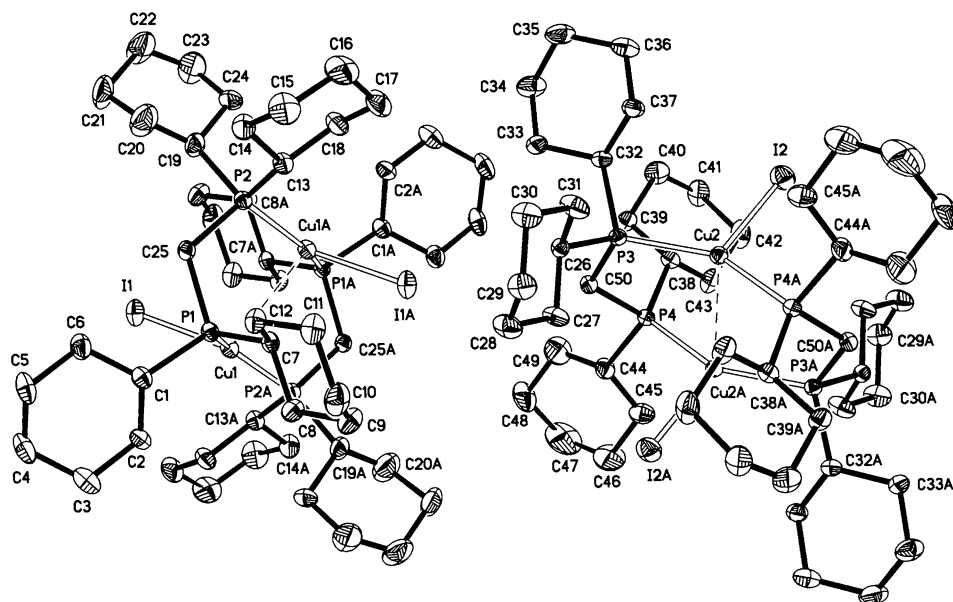


Figure 2. Structure of $[(\text{CuI})_2(\text{dcpm})_2]$ (perspective drawing; the thermal ellipsoids are drawn at 40% probability).

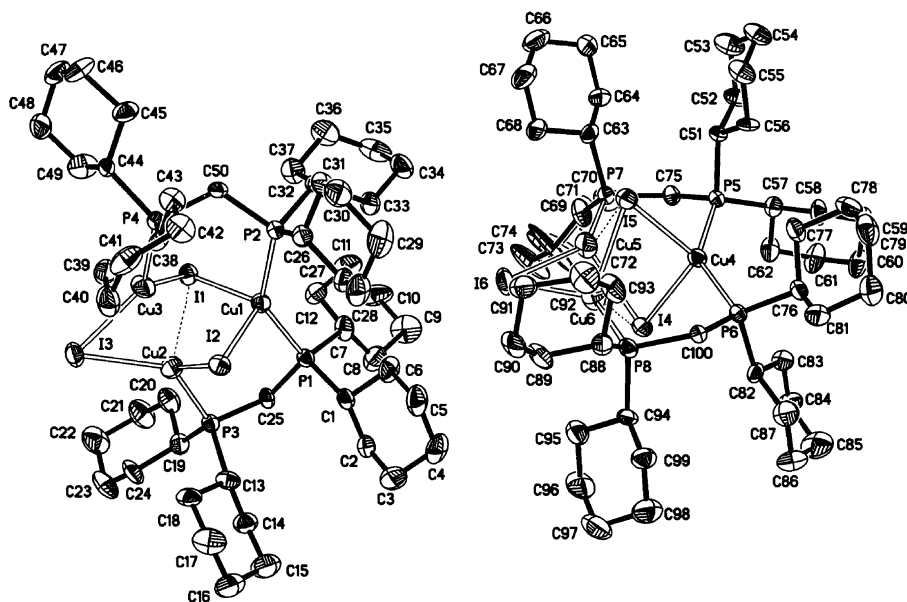


Figure 3. Structure of $[(\text{CuI})_3(\text{dcpm})_2]$ (perspective drawing; the thermal ellipsoids are drawn at 40% probability). The shortest $\text{Cu}\cdots\text{Cu}$ distance is 2.475(1) Å.

the 240–320 nm spectral region could be obscured by the absorption of the iodide anion. In such cases, a definitive spectroscopic assignment remains difficult. Complex **2** in acetonitrile is characterized by the absorption band at 319 nm, which is red-shifted from the 309 nm band in dichloromethane solution. This is ascribed to the formation of $[\text{Cu}_2(\text{dcpm})_2(\text{CH}_3\text{CN})_2]^{2+}$ (Figure 5). The UV/Vis absorption spectra of **1** and **2** in dichloromethane show an intense absorption band at 309 nm with large extinction coefficient ($\geq 10^4 \text{ mol}^{-1} \text{ dm}^3 \text{ cm}^{-1}$). Based on previous studies,^[6b] this band is assigned to the metal–metal $3d\sigma^* \rightarrow 4p\sigma$ transition. In dichloromethane solutions, the absorption spectra of complexes **3–5** have no distinctive features. However in

acetonitrile solutions, there is a distinct absorption that appears as a shoulder with λ_{max} at 308–315 nm (Figure 6). We tentatively suggest that the lower energy absorption in complexes **3–5** is due to electronic transitions that involve a $\text{Cu}^{\text{I}}\text{–Cu}^{\text{I}}$ interaction and $\text{I}^- \rightarrow \text{Cu}^+$ charge transfer in the excited state.

Emission spectra: Upon excitation at 290 nm, solid samples of **1**, **2**, and **5** display intense photoluminescence with λ_{max} at 460 ($\tau=36$), 377 ($\tau=63$) and 474 ($\tau=58$), and 456 nm ($\tau=9 \mu\text{s}$) at room temperature, respectively (Figures 7 and 8), corresponding emission quantum yields of the powdered samples are 0.26, 0.42, and 0.56. The results are listed in Table 3. The emission properties of **5** have been discussed previously.^[6b] Complex **2** has a short Cu–Cu distance (2.6905 Å); thus, the high energy emission at 377 nm could be attributed to the triplet emission from the Cu–Cu-bonded $^3[3d\sigma^*4p\sigma]$ excited state and the lower-energy emission at 474 nm to complexation of BF_4^- to the $[\text{Cu}_2(\text{dcpm})_2]^{2+}$ core in the excited state. This assignment is based on investigations of the spectroscopic features and the crystal structures determined for these complexes.

Compared to the emissions of **1**, **2**, and **5**, solid samples of **3** and **4** show lower-energy emissions with λ_{max} at 626 and 590 nm at room temperature, respectively (Figure 8). The emissions have lifetimes on the microsecond time scale, implying that these emissions are from the triplet excited states. With reference to previous work on a series of polynuclear copper(I) complexes,^[13,24] these emissions could be ascribed to excited states with a mixture of $3d \rightarrow 4p$ and iodide-to-metal charge transfer parentage. The solid-state emission spectra of **3** and **4** are markedly temperature-dependent. In contrast to only one emission band at room temperature, two emission bands with peak maxima at 480 and 680 nm for **3**, and 490 and 650 nm for **4** are observed at 77 K (Figure 8). This is similar to the solid emission of the related $[\text{Cu}_4\text{L}_4]$ complex (L=pyridine) reported by Ford and co-workers,^[13a] but different from the emission of

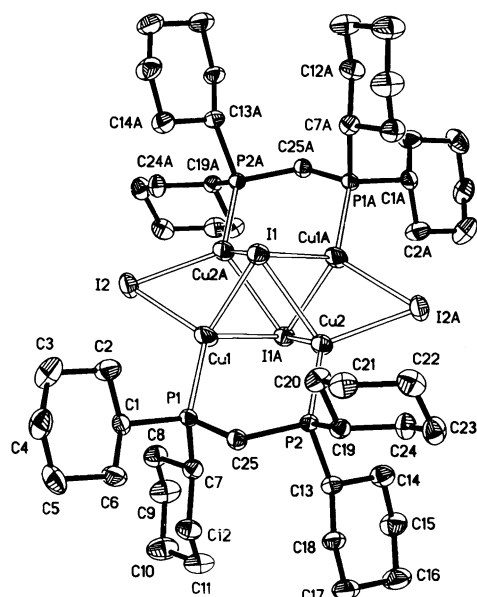


Figure 4. Structure of $[(\text{CuI})_4(\text{dcpm})_2]$ (perspective drawing; the thermal ellipsoids are drawn at 40% probability).

$[\text{Cu}_4\text{I}_4\text{L}_4]$ ($\text{L} = \text{piperidine}$ or morpholine) which display only a single emission band at 77 K.^[1a] The emission of **3** and **4** could be related to the short Cu–Cu contact distances of 2.4748 and 2.5758 Å; the high-energy emission originates

from a triplet metal-centered $3d \rightarrow (4s, 4p)$ excited state modified by a $\text{Cu} \cdots \text{Cu}$ interaction.

All complexes display intense emissions with long lifetimes in 77 K glassy solutions. At room temperature, solutions of the complexes in acetonitrile showed only weak emission in the 470–520 nm region (Figure 9); the emission quantum yields are $2\text{--}4 \times 10^{-3}$. In dichloromethane solutions, no emission was found for **1** or **2**, and excitation of **3** or **4** at 320 nm gave a red emission (Table 3 and Figure 9). In acetone solutions a red emission with λ_{max} at 625 nm was recorded for **1** or **2** (Figure 10). The large Stokes shift between the emission (625 nm) and absorption (320 nm) energies deserves attention. Based on the reported crystal structure of $[\text{Cu}_2(\text{naph})_2(\text{Me}_2\text{CO})](\text{PF}_6)_2$,^[25] we propose that $(\text{CH}_3)_2\text{CO}$ would coordinate to the $[\text{Cu}_2(\text{dcpm})_2]^{2+}$ core in the excited state. Such exciplex formation is suggested to be responsible for the red emission. However, attempts to obtain acetone adducts of $[\text{Cu}_2(\text{dcpm})_2]^{2+}$ were unsuccessful.

Time-resolved absorption spectra: The time-resolved absorption difference spectra of acetonitrile solutions of **1–5** were recorded following flash photolysis at 266 nm. As depicted in Figure 11, the spectra show absorption peaks with λ_{max} at 340–410 and 850–870 nm. The spectral data are listed in Table 3. Comparison of the decay lifetimes of absorption signals for **3–5** with the corresponding emission lifetimes imply the generation of new species upon laser flash photolysis. However, for acetone solutions of **1** or **2**, the decay lifetimes of the absorption signals at about 370 and 880 nm, re-

Table 3. Spectroscopic and photophysical properties of **1–5**.

Complex	Medium (T [K])	$\lambda_{\text{abs}}[\text{nm}]$ (ϵ [$\text{mol}^{-1}\text{dm}^3\text{cm}^{-1}$])	$\lambda_{\text{em}}[\text{nm}]/\tau[\mu\text{s}]$	${}^{[c]}\lambda_{\text{abs}}[\text{nm}]/\tau[\mu\text{s}]$	ϕ_{em}
1	CH_3CN (298)	263 (6155), 319 (6047)	475/3.6	380/4.9, 400/4.8, 850/5.6	0.004
	CH_2Cl_2 (298)	231 (12356), 309 (13107)	non-emissive		
	$(\text{CH}_3)_2\text{CO}$ (298)		625/4.3	370/4.4, 440/4.3, 880/4.5	
	glass (77) ^[b]		415/126		
	solid (298)		460/36		0.26
2	CH_3CN (298)	263 (5883), 319 (5830)	480/4.9		
	CH_2Cl_2 (298)	231 (13901), 309 (15062)	non-emissive		
	$(\text{CH}_3)_2\text{CO}$ (298)	328 (3004)	625/4.4	370/4.5, 440/4.3, 880/4.1	0.015
	glass (77) ^[b]		415/127		
	solid (298)		377/63, 474/58		0.42
5	CH_3CN (298)	243 (28790), 279 (7085)	466/3.7	360/12, 400/15	
		312(sh) (6470)		870/16	
	CH_2Cl_2 (298)	238 (43390), 279 (11320), 321 (6466)		480/0.17	0.003
	glass (77) ^[b]		453/17		
	solid (298)		456/8.9		0.56
3	CH_3CN (298)	245 (20518), 277 (3644), 308(sh) (1596)	500/2.8, 660/2.5	360/6.0, 380/7.6, 410/11, 860/11	0.002
	CH_2Cl_2 (298)	244(sh) (37265), 287 (6776)	690/3.7		0.008
	glass (77) ^[a]		430/15, 480/87, 630/81		
	solid (298)		626/10		0.11
	solid (77)		480/11, 680/25		
4	CH_3CN (298)	245 (46984), 277(sh) (6252), 315(sh) (2052)	520/1.6, 660/1.4	340/4.4, 390/4.0, 860/4.9	0.004
	CH_2Cl_2 (298)	248(sh) (39296)	700/0.27, 3.23		0.003
	glass (77) ^[a]		485/80		
	solid (298)		590/9.7		0.12
	solid (77)		490/7.4, 650/9.7		

[a] solvent: $\text{CH}_3(\text{CH}_2)_2\text{CN}$. [b] EtOH/MeOH (v/v, 1/4). [c] decay lifetime of transient difference absorption signals; sh = shoulder

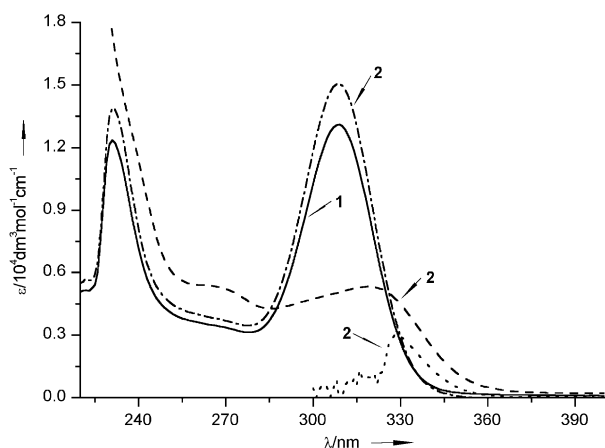


Figure 5. UV/Vis absorption spectra of $[\text{Cu}_2(\text{dcpm})_2(\text{CH}_3\text{CN})_2](\text{BF}_4)_2$ (**1**) in dichloromethane, and $[\text{Cu}_2(\text{dcpm})_2](\text{BF}_4)_2$ (**2**) in acetonitrile (dash line), dichloromethane (dash dot line), and acetone (dot line) at room temperature.

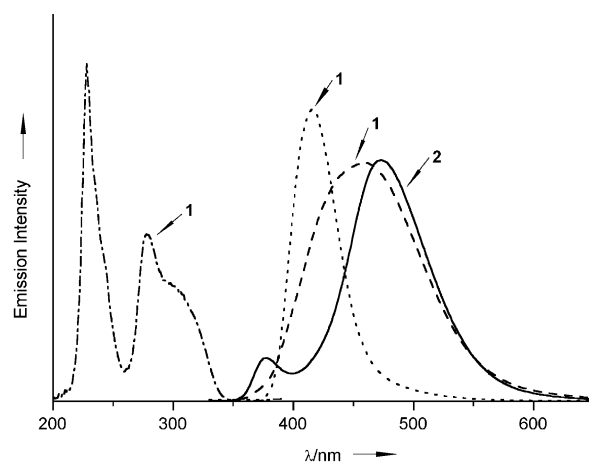


Figure 7. Room-temperature solid-state emission spectra (excitation at 290 nm) of $[\text{Cu}_2(\text{dcpm})_2(\text{CH}_3\text{CN})_2](\text{BF}_4)_2$ (**1**) (dash line) and $[\text{Cu}_2(\text{dcpm})_2](\text{BF}_4)_2$ (**2**) (solid line); excitation (dash dot line) and emission (dot line) spectra of $[\text{Cu}_2(\text{dcpm})_2(\text{CH}_3\text{CN})_2](\text{BF}_4)_2$ (**1**) in EtOH/MeOH (1/4) at 77 K.

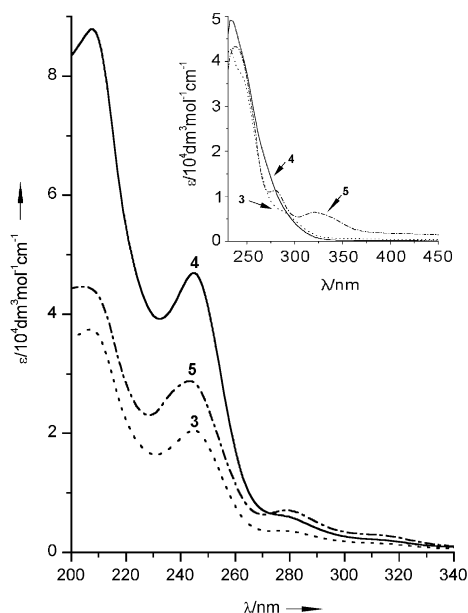


Figure 6. UV/Vis absorption spectra of $[(\text{CuI})_3(\text{dcpm})_2]$ (**3**), $[(\text{CuI})_4(\text{dcpm})_2]$ (**4**), and $[(\text{CuI})_2(\text{dcpm})_2]$ (**5**) in acetonitrile at room temperature. Inset: in dichloromethane.

spectively, match the corresponding emission lifetimes, suggesting that the absorption signals and emission come from the same triplet excited state (Figure 12). The results described above could rule out the possibility that the high- or low-energy transient absorption originate from either the metal–metal $^3(3d\sigma^* \rightarrow 4p\sigma)$ excited state of coordinated complexes of solvent for complexes **1** and **2** or with a mixed $3d\sigma^* \rightarrow 4p\sigma/\text{LMCT}$ triple excited state for complexes **3–5**. In the complexes, strong excited-state distortion should increase the Cu–Cu bonding, and for mononuclear copper(I) complexes no transient absorption has been observed in the range.^[14,5,19a,26]

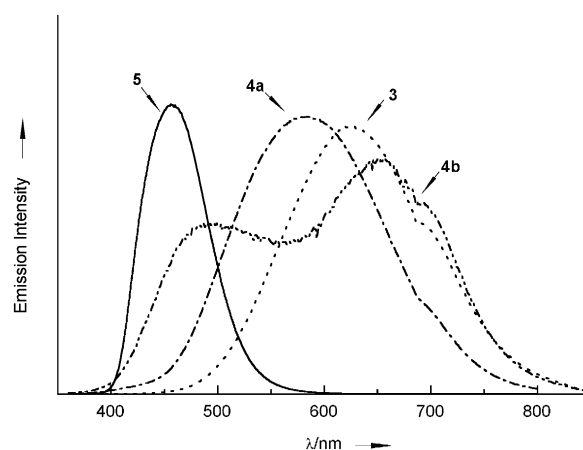


Figure 8. Solid-state emission spectra of $[(\text{CuI})_3(\text{dcpm})_2]$ (**3**), $[(\text{CuI})_4(\text{dcpm})_2]$ (**4a**), and $[(\text{CuI})_2(\text{dcpm})_2]$ (**5**) with excitation at 320 nm at 298 K, $[(\text{CuI})_4(\text{dcpm})_2]$ (**4b**) at 77 K.

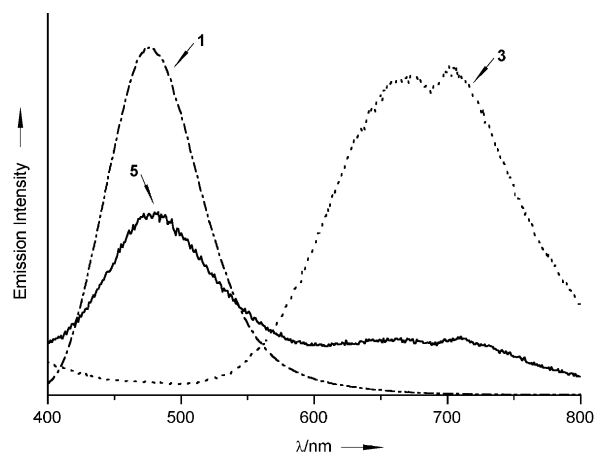


Figure 9. Emission spectra of $[(\text{CuI})_3(\text{dcpm})_2]$ (**3**) and $[(\text{CuI})_2(\text{dcpm})_2]$ (**5**) in degassed dichloromethane, and $[\text{Cu}_2(\text{dcpm})_2(\text{CH}_3\text{CN})_2](\text{BF}_4)_2$ (**1**) in degassed acetonitrile with excitation at 320 nm at 298 K.

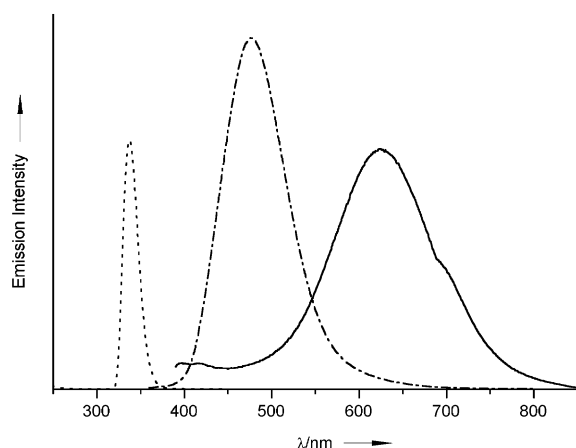


Figure 10. Emission spectra of $[\text{Cu}_2(\text{dcpm})_2](\text{BF}_4)_2$ with excitation at 320 nm in degassed acetone (solid line) and in degassed acetonitrile (dash dot line), excitation spectrum in degassed acetone (dotted line) at 298 K.

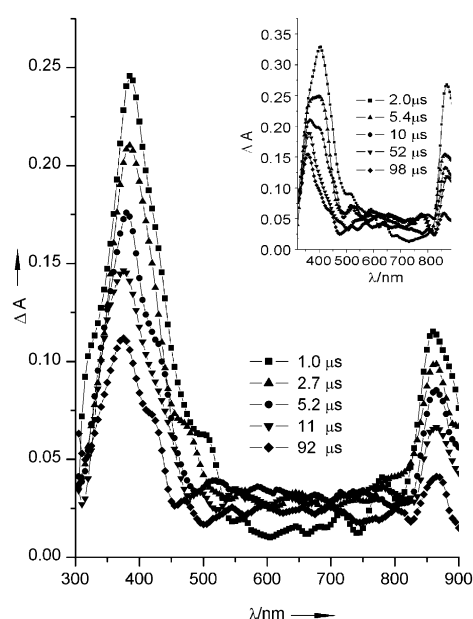


Figure 11. Room-temperature time-resolved difference absorption spectra of $[(\text{CuI})_3(\text{dcpm})_2]$ ($1.7 \times 10^{-5} \text{ M}$) recorded at 1, 2.7, 5.2, 11, and 92 μs after excitation at 266 nm in degassed acetonitrile. Inset: room-temperature time-resolved difference absorption spectra of $[(\text{CuI})_2(\text{dcpm})_2]$ ($1.8 \times 10^{-5} \text{ M}$) monitored after 1.5 μs pulsed excitation at 266 nm in degassed acetonitrile.

Experimental Section

Materials: CuI (Aldrich) and dcpm (Strem) were used as received. Solvents (HPLC grade) used in the spectroscopic measurements were dried and distilled under an argon atmosphere prior to use.

$[\text{Cu}_2(\text{dcpm})_2(\text{CH}_3\text{CN})_2](\text{BF}_4)_2$ (1), $[\text{Cu}_2(\text{dcpm})_2](\text{BF}_4)_2$ (2): An equimolar mixture of $[\text{Cu}(\text{CH}_3\text{CN})_4](\text{BF}_4)_2$ and dcpm was dissolved in dichloromethane (15 mL) at room temperature. After stirring for 2 h, the mixture was filtered. Upon removal of solvent by rotary evaporation, the product $[\text{Cu}_2(\text{dcpm})_2](\text{BF}_4)_2$ was obtained as a white solid. The solid was recrystallized from dichloromethane by slow evaporation. Complexes **1** and **2** were obtained as crystalline solids by diffusion of diethyl ether into a solution of $[\text{Cu}_2(\text{dcpm})_2](\text{BF}_4)_2$ in acetonitrile or acetone, respectively. The crystalline solid was characterized by ^{31}P NMR and X-ray crystallogra-

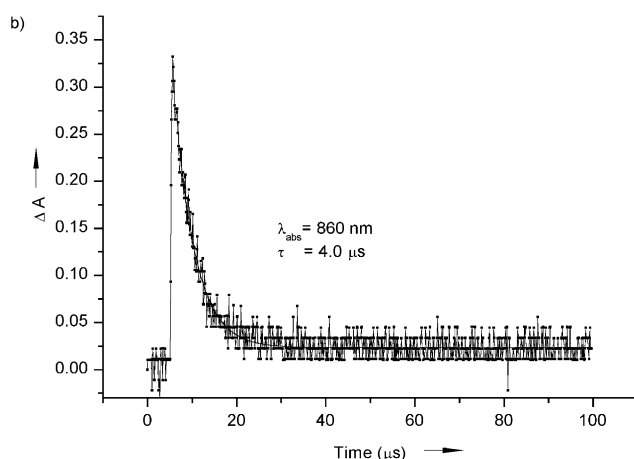
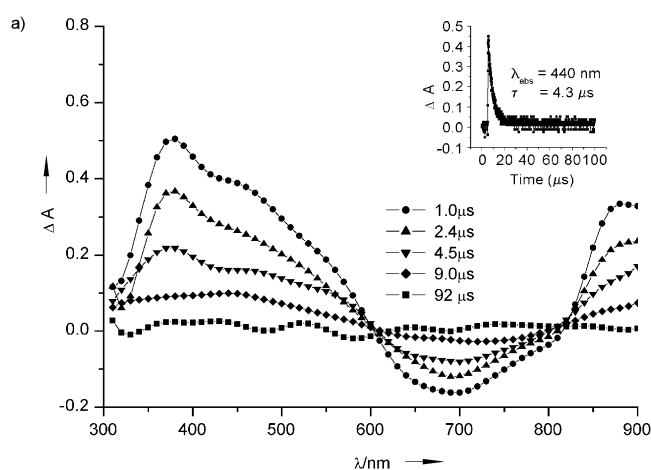


Figure 12. a) Room-temperature time-resolved difference absorption spectra of $[\text{Cu}_2(\text{dcpm})_2](\text{BF}_4)_2$ ($8.0 \times 10^{-5} \text{ M}$) recorded at 1.0, 2.4, 4.5, 9.0, and 92 μs after excitation at 355 nm in degassed acetone. Inset: decay traces of transient difference absorption spectra of $[\text{Cu}_2(\text{dcpm})_2](\text{BF}_4)_2$ monitored at 440 nm; b) monitored at 860 nm.

phy. ^{31}P NMR (202 MHz, CD_3CN , 298 K): $\delta = 9.8$ ppm for **1**; (CDCl_3): $\delta = 16.5$ ppm; (CD_3CN): $\delta = 9.8$ ppm; ($(\text{CD}_3)_2\text{CO}$): $\delta = 19.8$ ppm for **2**.

$[(\text{CuI})_3(\text{dcpm})_2]$ (3): dcpm was added to a suspension of CuI in dichloromethane (25 mL), and the mixture was stirred for 4 h at room temperature. The resulting solution was filtered and concentrated down to 3 mL. Addition of diethyl ether gave the product as a white solid. Recrystallization by slow diffusion of diethyl ether into a solution of the crude product in dichloromethane gave colorless crystals. The crystalline solid was characterized by ^{31}P NMR and X-ray crystallography. ^{31}P NMR (202 MHz, CDCl_3 , 298 K): $\delta = -2.0$ and -2.7 ppm.

$[(\text{CuI})_4(\text{dcpm})_2]$ (4): The preparation of $[(\text{CuI})_4(\text{dcpm})_2]$ (**4**) was similar to that of **3**. A mixture of CuI and dcpm (2:1 molar ratio) in dichloromethane (40 mL) was stirred for 5 h at room temperature. The reaction mixture was concentrated in vacuum and the crude product was recrystallized from a CH_2Cl_2 /diethyl ether mixture to give colorless crystals. The crystalline solid was characterized by ^{31}P NMR and X-ray crystallography. ^{31}P NMR (202 MHz, CDCl_3 , 298 K): $\delta = -3.1$ ppm.

Equipment and procedure: Steady-state absorption spectra were recorded at ambient temperature with a HITACHI U-3010 UV/Vis spectrophotometer. Crystals of a suitable size were mounted either on glass fibers or in capillary tubes. X-ray data were collected either on a MAR PSD diffractometer or Rigaku AFC7R diffractometer. Intensity data were collected by the ω - 2θ scan technique. The images were interpreted and integrated by using the DENZO or ABSOR programs. The structures were solved by direct (SIR92) or Patterson methods (PATTY) and expanded by the Fourier method. Structural refinement on F or F^2 by full-matrix least-squares analysis was performed by using TeXsan, SHELXL-93, or

NRCC-SDP VAX programs. The ORTEP drawings of the structures were displayed with hydrogen atoms omitted for clarity. The unweighted and weighted agreement factors (R_f , R_w) and the goodness of fit (S) were calculated.

CCDC-224323 (1), CCDC-224324 (2), CCDC-224325 (3), CCDC-224326 (4) contain the supplementary crystallographic data for this paper. These data can be obtained free of charge via www.ccdc.cam.ac.uk/conts/retrieving.html (or from the Cambridge Crystallographic Centre, 12 Union Road, Cambridge CB21EZ, UK; Fax: (+44)1223-336033; or deposit@ccdc.cam.ac.uk).

Corrected emission and excitation spectra were obtained on a HITACHI F-4500 fluorescence spectrofluorometer adapted to a right-angle configuration. The emission spectra were corrected for detector response and the excitation spectra were corrected for optical path difference between the light source and the sample with programs and data supplied by the manufacturer. Suitable bandpass filters were used to cut off the second harmonic of the monochromatic excitation light source and stray light. Solutions for excitation or emission measurements were degassed by employing at least four freeze-pump-thaw cycles. Low-temperature (77 K) emission spectra for glass and solid-state samples were recorded in quartz tubes (5 mm diameter) that were placed inside a liquid nitrogen bath contained in a quartz optical Dewar flask.

Emission quantum yields in different solvents were determined relative to quinine sulfate in 1.0 N sulfuric acid at low concentrations ($\Phi_{em} = 0.546$) or $[Ru(bpy)_3]^{2+}$ ($\Phi_{em} = 0.042$).^[27] Measurement of emission quantum yields of powdered samples involved determination of the diffuse reflectance spectra of 1–4 relative to KBr at the excitation wavelength.^[28] The measured results were corrected for the detector response as a function of wavelength. Emission lifetimes of solid or solution samples were performed with a Quanta Ray DCR-3 Nd-YAG laser with a pulse-width of 8 ns and an excitation wavelength of 266 nm (fourth harmonic). Emission signals were collected at right angles to the excitation pulse by a Hamamatsu R928 photomultiplier tube and recorded on a Tektronix model 2430 digital oscilloscope.

Transient absorption spectra were recorded after excitation of the sample in degassed acetonitrile with an 8 ns laser pulse at 266 nm or in degassed acetone at 355 nm. The monitoring beam was provided by a 300 W continuous-wave xenon lamp oriented perpendicular to the direction of the laser pulse. The transient absorption signals at each wavelength were collected with a SpectraPro-275 monochromator operated with 2 mm slits, and the signal was fed to a Tektronix TDS 520D oscilloscope. The optical difference spectrum was generated point by point by monitoring the signal at individual wavelengths.

Acknowledgment

This work was supported by the National Natural Science Foundation of China (50273045, 90210033). We thank the Chinese Government for support of the Chinese Academy of Science Hundred Talents and the foundation (2001E0005Z) for Key Project of Yunnan Provincial Science and Technology Commission, the University of Hong Kong, and the Hong Kong Research Grants Council for financial support.

- [1] a) P. C. Ford, A. Vogler, *Acc. Chem. Res.* **1993**, *26*, 220–226; b) J. A. Simon, W. E. Palke, P. C. Ford, *Inorg. Chem.* **1996**, *35*, 6413–6421; c) E. Cariati, J. Bourassa, P. C. Ford, *Chem. Commun.* **1998**, 1623–1624; d) P. C. Ford, E. Cariati, J. Bourassa, *Chem. Rev.* **1999**, *99*, 3625–3647; e) E. Cariati, X. H. Bu, P. C. Ford, *Chem. Mater.* **2000**, *12*, 3385–3391; f) M. Vitale, P. C. Ford, *Coord. Chem. Rev.* **2001**, *219–221*, 3–16.
- [2] a) V. W. W. Yam, W. K. M. Fung, K. K. Cheung, *Angew. Chem.* **1996**, *108*, 1213–1215; *Angew. Chem. Int. Ed. Engl.* **1996**, *35*, 1100–1102; b) V. W. W. Yam, K. K. W. Lo, C. R. Wang, K. K. Cheung, *J. Phys. Chem.* **1997**, *101*, 4666–4672; c) V. W. W. Yam, W. K. M. Fung, K. K. Cheung, *Organometallics* **1998**, *17*, 3293–3298; d) V. W. W. Yam, K. K. W. Lo, *Chem. Soc. Rev.* **1999**, *28*, 323–334; e) V. W. W. Yam, E. C. C. Cheng, N. Y. Zhu, *Chem. Commun.* **2001**, 1028–1029.
- [3] a) D. R. McMillin, K. M. McNett, *Chem. Rev.* **1998**, *98*, 1201–1219; b) C. T. Cunningham, K. L. H. Cunningham, J. F. Michalec, D. R. McMillin, *Inorg. Chem.* **1999**, *38*, 4388–4392; c) P. Lugo-Ponce, D. R. McMillin, *Coord. Chem. Rev.* **2000**, *208*, 169–191; d) C. T. Cunningham, J. J. Moore, K. L. H. Cunningham, P. E. Fanwick, D. R. McMillin, *Inorg. Chem.* **2000**, *39*, 3638–3644.
- [4] a) K. M. Merz, Jr., R. Hoffmann, *Inorg. Chem.* **1988**, *27*, 2120–2127; b) J. D. Barrie, B. Dunn, G. Hollingsworth, J. I. Zink, *J. Phys. Chem.* **1989**, *93*, 3958–3963; c) X. Y. Liu, F. Mota, P. Alemany, J. J. Novoa, S. Alvarez, *Chem. Commun.* **1998**, 1149–1150; d) P. Pyykkö, P. Mendizabal, *Inorg. Chem.* **1998**, *37*, 3018–3025; e) Y. Rondelez, O. Sénéque, M. N. Rager, A. F. Duprat, O. Reinaud, *Chem. Eur. J.* **2000**, *6*, 4218–4226.
- [5] a) D. V. Scaltrito, C. A. Kelly, M. Ruthkosky, M. C. Zarus, G. J. Meyer, *Inorg. Chem.* **2000**, *39*, 3765–3770; b) H. Xu, J. H. K. Yip, *Inorg. Chem.* **2003**, *42*, 4492–4494; c) J. Cody, J. Dennisson, J. Gilmore, D. G. VanDerveer, M. M. Henary, A. Gabrielli, C. D. Sherrill, Y. Zhang, C. P. Pan, C. Burda, C. J. Fahrni, *Inorg. Chem.* **2003**, *42*, 4918–4929.
- [6] a) W. H. Chan, Z. Z. Zhang, T. C. W. Mak, C. M. Che, *J. Organomet. Chem.* **1998**, *556*, 169–172; b) C. M. Che, Z. Mao, V. M. Miskowski, M. C. Tse, C. K. Chan, K. K. Cheung, D. L. Phillips, K. H. Leung, *Angew. Chem.* **2000**, *112*, 4250–4254; *Angew. Chem. Int. Ed.* **2000**, *39*, 4084–4088; c) Z. Mao, H. Y. Chao, Z. Hui, C. M. Che, W. F. Fu, K. K. Cheung, N. Y. Zhu, *Chem. Eur. J.* **2003**, *9*, 2885–2897.
- [7] a) J. Díez, M. P. Gamasa, J. Gimeno, E. Lastra, A. Aguirre, S. García-Granda, *Organometallics* **1993**, *12*, 2213–2220; b) V. W. W. Yam, W. K. Lee, K. K. Cheung, *J. Chem. Soc. Dalton Trans.* **1996**, 2335–2339; c) J. Díez, M. P. Gamasa, J. Gimeno, A. Aguirre, S. García-Granda, J. Holubova, L. R. Falvello, *Organometallics* **1999**, *18*, 662–669.
- [8] a) C. Bonnefous, N. Bellec, R. P. Thummel, *Chem. Commun.* **1999**, 1243–1244; b) J. Zhang, R. G. Xiong, J. L. Zuo, X. Z. You, *Chem. Commun.* **2000**, 1495–1496.
- [9] a) M. T. Miller, T. B. Karpishin, *Inorg. Chem.* **1999**, *38*, 5246–5249; b) X. M. Zhang, M. L. Tong, X. M. Chen, *Angew. Chem.* **2002**, *114*, 1071–1073; *Angew. Chem. Int. Ed.* **2002**, *41*, 1029–1031; c) G. S. Papaefstathiou, L. R. MacGillivray, *Angew. Chem.* **2002**, *114*, 2174–2177; *Angew. Chem. Int. Ed.* **2002**, *41*, 2070–2073.
- [10] a) W. S. Striejewske, R. R. Conry, *Chem. Commun.* **1998**, 555–556; b) H. W. Yim, L. M. Tran, E. E. Pullen, D. Rabinovich, L. M. Liable-Sands, T. E. Cincolino, A. L. Rheingold, *Inorg. Chem.* **1999**, *38*, 6234–6239; c) Y. Shimazaki, H. Yokoyama, O. Yamauchi, *Angew. Chem.* **1999**, *111*, 2561–2563; *Angew. Chem. Int. Ed.* **1999**, *38*, 2401–2402; d) D. V. Scaltrito, H. C. Fry, B. M. Showalter, D. W. Thompson, H. C. Liang, C. X. Zhang, R. M. Kretzer, E. I. Kim, J. P. Toscano, K. D. Karlin, G. J. Meyer, *Inorg. Chem.* **2001**, *40*, 4514–4515; e) C. Ohrenberg, L. M. Liable-Sands, A. L. Rheingold, C. G. Riordan, *Inorg. Chem.* **2001**, *40*, 4276–4283; f) J. M. Vincent, C. Philouze, I. Pianet, J. B. Verlhac, *Chem. Eur. J.* **2000**, *6*, 3595–3599.
- [11] a) S. Kitagawa, M. Munakata, H. Shimono, S. Matsuyama, H. Masuda, *J. Chem. Soc. Dalton Trans.* **1990**, 2105–2109; b) S. Kitagawa, S. Kawata, Y. Nozaka, M. Munakata, *J. Chem. Soc. Dalton Trans.* **1993**, 1399–1404; c) K. Singh, J. R. Long, P. Stavropoulos, *J. Am. Chem. Soc.* **1997**, *119*, 2942–2943; c) R. D. Willett, B. Twamley, *Inorg. Chem.* **2001**, *40*, 6502–6505.
- [12] a) Q. T. Anderson, E. ErKizia, R. R. Conry, *Organometallics* **1998**, *17*, 4917–4920; b) S. Haddad, R. D. Willett, *Inorg. Chem.* **2001**, *40*, 809–811; c) D. G. Cuttill, S. M. Kuang, P. E. Fanwick, D. R. McMillin, R. A. Walton, *J. Am. Chem. Soc.* **2002**, *124*, 6–7.
- [13] a) K. R. Kyle, C. K. Ryu, J. A. DiBenedetto, P. C. Ford, *J. Am. Chem. Soc.* **1991**, *113*, 2954–2965; b) C. K. Ryu, M. Vitale, P. C. Ford, *Inorg. Chem.* **1993**, *32*, 869–874; c) D. Tran, J. L. Bourassa, P. C. Ford, *Inorg. Chem.* **1997**, *36*, 439–442.
- [14] a) K. H. Leung, D. L. Phillips, M. C. Tse, C. M. Che, V. M. Miskowski, *J. Am. Chem. Soc.* **1999**, *121*, 4799–4803; b) W. F. Fu, K. C. Chan, V. M. Miskowski, C. M. Che, *Angew. Chem.* **1999**, *111*, 2953–2955; *Angew. Chem. Int. Ed.* **1999**, *38*, 2783–2785; c) C. M. Che, M. C. Tse, M. C. W. Chan, K. K. Cheung, D. L. Phillips, K. H. Leung, *J. Am. Chem. Soc.* **2000**, *122*, 2464–2468; d) W. F. Fu, K. C. Chan, K. K. Cheung, C. M. Che, *Chem. Eur. J.* **2001**, *7*, 4656–4664.

- [15] J. Beck, J. Strähle, *Angew. Chem.* **1985**, *97*, 419–420; *Angew. Chem. Int. Ed. Engl.* **1985**, *24*, 409–410.
- [16] a) P. K. Mehrotra, R. Hoffmann, *Inorg. Chem.* **1978**, *17*, 2187–2189; b) F. A. Cotton, X. Feng, M. Matusz, R. Poli, *J. Am. Chem. Soc.* **1988**, *110*, 7077–7083; c) C. Kölmel, R. Ahlrichs, *J. Phys. Chem.* **1990**, *94*, 5536–5542; d) U. Siemeling, U. Vorfeld, B. Neumann, H. G. Stammer, *Chem. Commun.* **1997**, 1723–1724; e) J. M. Poblet, M. Bénard, *Chem. Commun.* **1998**, 1179–1180; f) H. L. Hermann, G. Boche, P. Schwerdtfeger, *Chem. Eur. J.* **2001**, *7*, 5333–5342.
- [17] J. M. Zuo, M. Kim, M. O'effe, J. C. H. Spence, *Nature*, **1999**, *401*, 49–52.
- [18] a) H. D. Hardt, A. Z. Pierre, *Z. Anorg. Allg. Chem.* **1973**, *402*, 107–112; b) V. Schramm, K. F. Fischer, *Naturwissenschaften*, **1974**, *61*, 500–501; c) M. R. Churchill, K. L. Kalra, *Inorg. Chem.* **1974**, *13*, 1065–1071; d) C. L. Raston, A. H. White, *J. Chem. Soc. Dalton Trans.* **1976**, 2153–2156.
- [19] a) A. Vogler, H. Kunkely, *J. Am. Chem. Soc.* **1986**, *108*, 7211–7212; b) M. Henery, J. I. Zink, *J. Am. Chem. Soc.* **1989**, *111*, 7407–7411; c) C. K. Ryu, K. R. Kyle, P. C. Ford, *Inorg. Chem.* **1991**, *30*, 3982–3986.
- [20] a) W. A. S. Goher, T. C. W. Mak, *Inorg. Chim. Acta* **1985**, *101*, L27–L30; b) L. M. Engelhardt, P. C. Healy, J. D. Kildea, A. H. White, *Aust. J. Chem.* **1989**, *42*, 185–199; c) P. M. Graham, R. D. Pike, *Inorg. Chem.* **2000**, *39*, 5121–5132; d) N. S. Persky, J. M. Chow, K. A. Poschmann, N. N. Lacuesta, S. L. Stoll, S. G. Bott, S. Obrey, *Inorg. Chem.* **2001**, *40*, 29–35.
- [21] P. F. Barron, J. C. Dyason, L. M. Engelhardt, P. C. Healy, A. H. White, *Inorg. Chem.* **1984**, *23*, 3766–3769.
- [22] J. E. Huheey, *Inorganic Chemistry: Principles of Structures and Reactivity*, 2nd ed., Harper and Row, New York, **1978**.
- [23] a) G. Nardin, L. Randaccio, E. Zangrando, *J. Chem. Soc. Dalton Trans.* **1975**, 2566–2569; b) J. K. Bera, M. Nethaji, A. G. Samuelson, *Inorg. Chem.* **1999**, *38*, 218–228.
- [24] a) N. P. Rath, E. M. Holt, K. Tanimura, *Inorg. Chem.* **1985**, *24*, 3934–3938; b) N. P. Rath, E. M. Holt, K. Tanimura, *J. Chem. Soc. Dalton Trans.* **1986**, 2303–2310.
- [25] M. Maekawa, M. Munakata, S. Kitagawa, T. Kuroda-Sowa, Y. Suenaga, M. Yamamoto, *Inorg. Chim. Acta* **1998**, *271*, 129–136.
- [26] A. Horváth, K. L. Stevenson, *Inorg. Chem.* **1993**, *32*, 2225–2227.
- [27] a) J. N. Demas, G. A. Crosby, *J. Phys. Chem.* **1971**, *75*, 991–1024; b) E. Amouyal, A. Homsy, J. C. Chambron, J. P. Sauvage, *J. Chem. Soc. Dalton Trans.* **1990**, 1841–1845.
- [28] M. S. Wrighton, D. S. Ginley, D. L. Morse, *J. Phys. Chem.* **1974**, *78*, 2229–2233.

Received: October 26, 2003 [F5657]